RADIOLOGY CASE REPORTS

Musculoskeletal

Magnetic resonance neurography in the diagnosis of a retroperitoneal ganglioneuroma: Case report and literature review

Cláudio Régis Sampaio Silveira MD[a,*], Clarissa Gadelha Maia Vieira MD[b],
Brenda Machado Pereira MD[b], Edson Lopes Junior MD[c], Gunter Gerson MD[d],
Daniel Gurgel Fernandes Távora MD[b], Avneesh Chhabra MD[e]

[a] Musculoskeletal Imaging Division, São Carlos Imaging/São Carlos Hospital, Fortaleza, CE, Brazil
[b] São Carlos Imaging, Rua Otoni Façanha de Sá, 69, Dionísio Torres, Fortaleza, Ceará, Brazil
[c] Neurosurgery Department, Geral Hospital of Fortaleza, Fortaleza, CE, Brazil
[d] Pathology Department, Federal University of Ceara, Fortaleza, CE, Brazil
[e] Radiology & Orthopaedic Surgery, UT Southwestern, Dallas, Texas

ARTICLE INFO

ABSTRACT

Magnetic resonance neurography is a technique for identifying anatomy and pathologic lesions of nerves, and has emerged as a helpful technique for localizing lesions and elucidating the underlying etiology. Ganglioneuromas are highly differentiated benign tumors. This lesion is rare and exhibits undetermined symptoms, the features of using the magnetic resonance neurography are a great ally to determine its diagnosis. The authors illustrate a case of retroperitoneal ganglioneuroma emphasizing its image characteristics using magnetic resonance neurography with the diagnosis confirmed by histopathological examination.

© 2018 the Authors. Published by Elsevier Inc. under copyright license from the University of Washington. This is an open access article under the CC BY-NC-ND license (http://creativecommons.org/licenses/by-nc-nd/4.0/).

Introduction

Technical aspects of magnetic resonance neurography (MRN) have been recently reviewed. Modern MRN uses high magnetic field strength (1.5 or 3 T) with high-resolution multiplanar structural sequences allowing the multiplanar representation of the lesions and demonstrates the relationships of the involved and displaced nerve roots. MRN can help localize lesions by directly observing nerve signal abnormalities, heterogeneous enhancement after the contrast, or by identifying myopathic changes in a particular nerve distribution; detect

incidental lesions mimicking neuropathic symptoms; or exclude neuropathy by revealing completely normal imaging characteristics of both muscle and nerve [1].

Neuroblastoma, ganglioneuroblastoma, and ganglioneuroma (GN) can be conceptualized as 3 maturational manifestations of a common neoplasm. GN is a differentiated ganglionic tumor that contains no immature neuroblastic elements [2].

GN, composed of mature ganglion cells, Schwann cells, and nerve fibers, is a rare tumor of neural crest origin in adolescence or young adulthood and can arise from the sympathetic ganglia and the adrenal medulla [3]. The 2 most common sites for GN are the retroperitoneum and the posterior mediastinum (approximately 90%), followed by the cervical region [4].

Since the appearance of neurographic sequences in the 1990s, MRN has become an essential part of the neuropathy diagnostic armamentarium. Because of technological advances through the development of new 3-dimensional (3D) imaging techniques, MRN is being increasingly used in the clinical routine for the evaluation of patients with plexopathies [5,6].

The authors illustrate an interesting case of retroperitoneal GN with histopathological and MRN appearances.

Case report

An 18-year-old woman sought emergency medical assistance in September 2015 with lumbar pain and progressive strength loss of lower limbs that had started 4 months ago. On physical examination, the patient was in good general condition, afebrile, oriented, and cooperative. On neurologic examination, she had bilateral paraparesis, asymmetric strength loss of the lower limbs, more accentuated on the right, and distally. There were also cauda equine symptoms of fecal retention and overflow urinary incontinence. Suspecting neurogenic cause, MRN of lumbosacral (LS) plexus was requested.

A high-field device (Philips Achieva 3.0T X-series magnetic resonance imaging (MRI) System; Philips Medical Systems, Best, The Netherlands) was used for LS plexus MRN. Spine and XL-torso coil were used with the following protocol: axial fast spin echo T1-weighted imaging, 3D volumetric T1- and T2-weighted imaging, axial spectral adiabatic inversion recovery T2-weighted imaging, 3D volumetric short tau inversion recovery imaging, 3D diffusion-weighted imaging (DWI), and 3D fat saturated (Fat-sat) T1-weighted gradient echo sequences both without contrast and after intravenous gadolinium injection. The images were post-processed at a workstation, and multiplanar reconstructions were generated using the thick-slab maximum intensity projection technique.

A large expansive neoplastic lesion occupying lumbar canal was seen from the middle of L1 vertebral body to the lower border of L4 vertebral body. The lesion was predominantly extradural (canalicular measurement—$11.0 \times 4.0 \times 2.0$ cm), presenting a heterogeneous hyperintense signal on T2-weighted and 3D short tau inversion recovery imaging, with low signal relative to the muscle signal on T1-weighted imaging (Figs. 1 and 2). On postcontrast imaging, there were areas of mild postcontrast heterogeneous and peripheral enhancement (Fig. 3). The lesion appeared multilobulated with smooth erosions and scalloping of the L2-4 vertebrae and multiple lumbar foramina (right > left). The dural sac was compressed and displaced anterolaterally to the left, the L1-3 nerves were engulfed, and L4-5 were displaced inferiorly (Fig. 4).

The lesion also presented a large right paravertebral component involving the ipsilateral psoas muscle with superior and anterolateral deviation of the right kidney and its ureter and slight ureteropelvic ectasia upstream. The measurements of right paravertebral component of the lesion are estimated to be $12.5 \times 7.0 \times 7.0$ cm (Fig. 5).

The histopathological study of the surgical specimen showed a solid, well-circumscribed, and compact tumor lesion with a brown and white, firm, and homogeneous cut surface. Microscopic analysis revealed biphasic neoplasia composed of scattered ganglion cells and grouped between abundant axonal
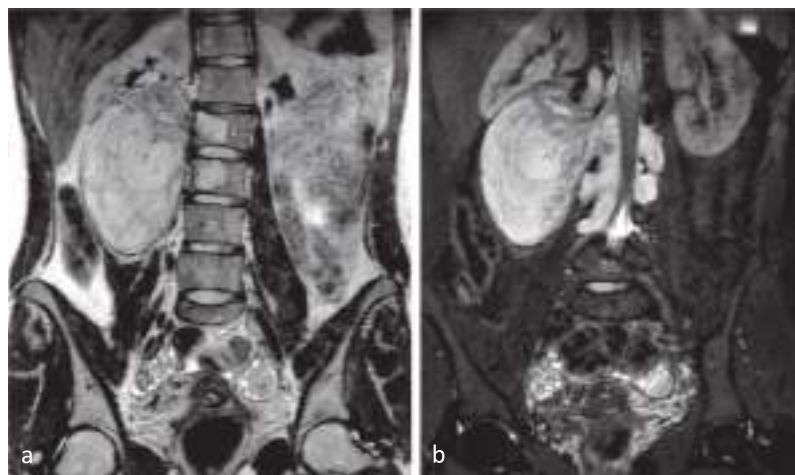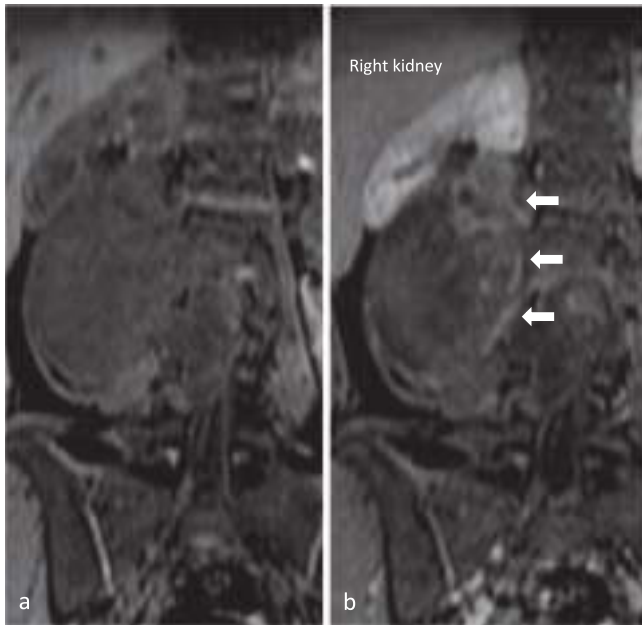

Fig. 1 – (A) T2-weighted 3-dimensional (3D) acquisition coronal and (B) 3D short tau inversion recovery coronal with reconstructions of the expansive lesion occupying the vertebral canal and the paravertebral component presenting a hyperintense heterogeneous signal with extensions into multiple neural foramina.
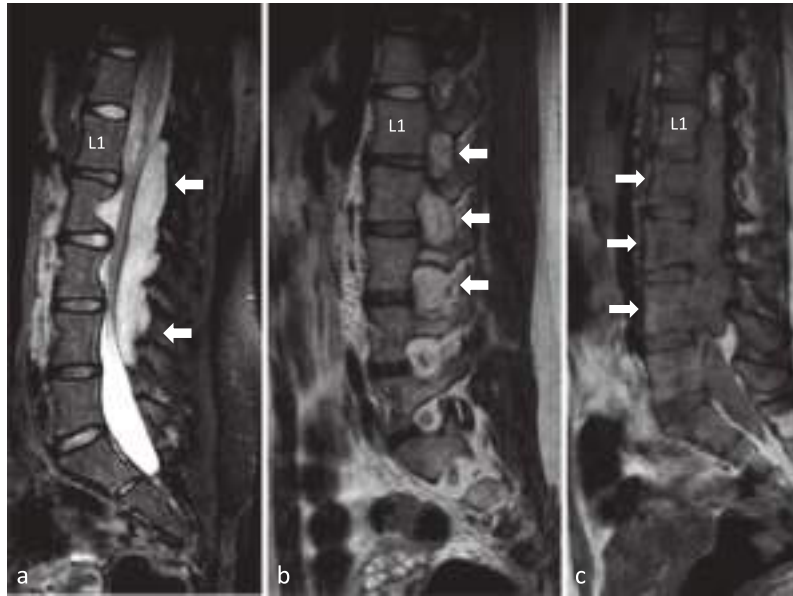
Fig. 2 – (A) 3-Dimensional (3D) short tau inversion recovery sagittal reconstruction showing the roots of the cauda equina grouped and diverted with thecal sac anteriorly. (B) T2-weighted 3D acquisition sagittal reconstruction demonstrating the lesion occupying the left foramina. (C) T1-weighted 3D acquisition sagittal reconstruction where the lesion determines erosion, infiltration, and scalloping of the L2, L3, and L4 vertebral bodies.

processes, sometimes accompanied by satellite cells and Schwann cells. In outbreaks, there were areas of hyalinization and fibrosis. There was no associated neuroblast or immature cells. Immunohistochemical reactions revealed strong marking by synaptophysin in ganglion cells and intense labeling by glial fibrillary acidic protein in axonal processes, Schwann cells, and satellite cells. Therefore, the immunophenotypic characteristics reveal a diagnosis of GN (Fig. 6).

Fig. 3 – (A) T1-weighted 3-dimensional (3D) acquisition coronal reconstruction imaging before and (B) and after intravenous administration of contrast. The lesion presents a large right paravertebral component with areas of mild postcontrast heterogeneous and peripheral enhancement displacing the kidney superolaterally.
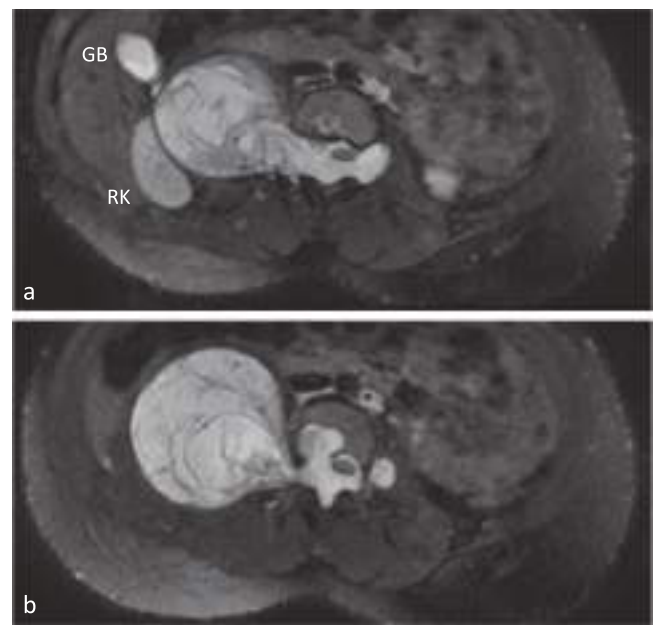
Fig. 4 – (A, B) T2-weighted spectral adiabatic inversion recovery axial reconstructions where the lesion determines erosion, infiltration, and scalloping of the L3 vertebral body, as well as widens the corresponding neural foramen crossing the midline. GB, gallbladder; RK, right kidney.
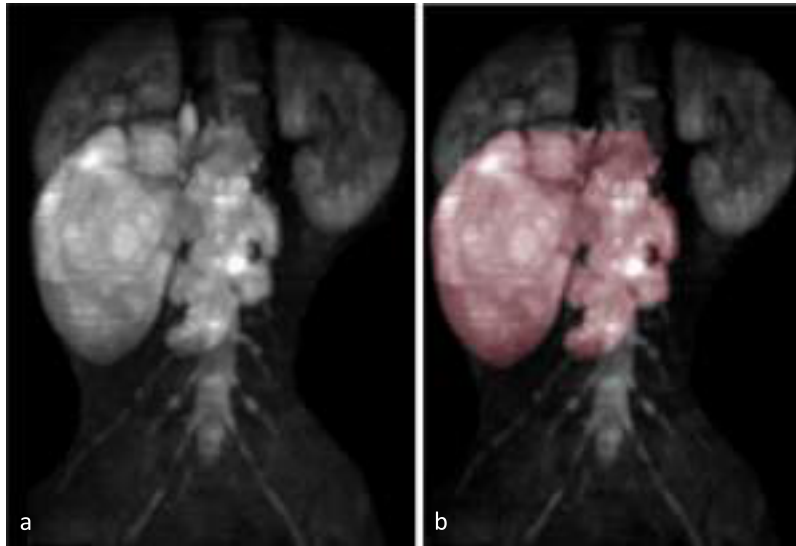
Fig. 5 – (A, B) 3-Dimensional diffusion-weighted magnetic resonance imaging with maximum intensity projection reconstruction coronal shows excellent vascular and background signal suppression with the large mass lesion engulfing bilateral L1-3 nerves and displacing the right L4 and L5 nerves.

Discussion

Lumbosacral plexus stems from the ventral branches of nerves L1 to L4 usually with a contribution from T12 nerve. It descends dorsally or inside the psoas muscle and provides lateral branches—iliohypogastric, ilioinguinal, genitofemoral, lateral femoral-cutaneous and femoral nerves, and medial branches—obturator nerve and lumbosacral trunk [4,6]. The evaluation of LS plexus and individual segments has become possible with advancement of the MRN techniques, especially 3D and diffusion imaging [7,8].

GN occurs in children and young adults [9]; the median age at diagnosis is approximately 7 years. There is a slight
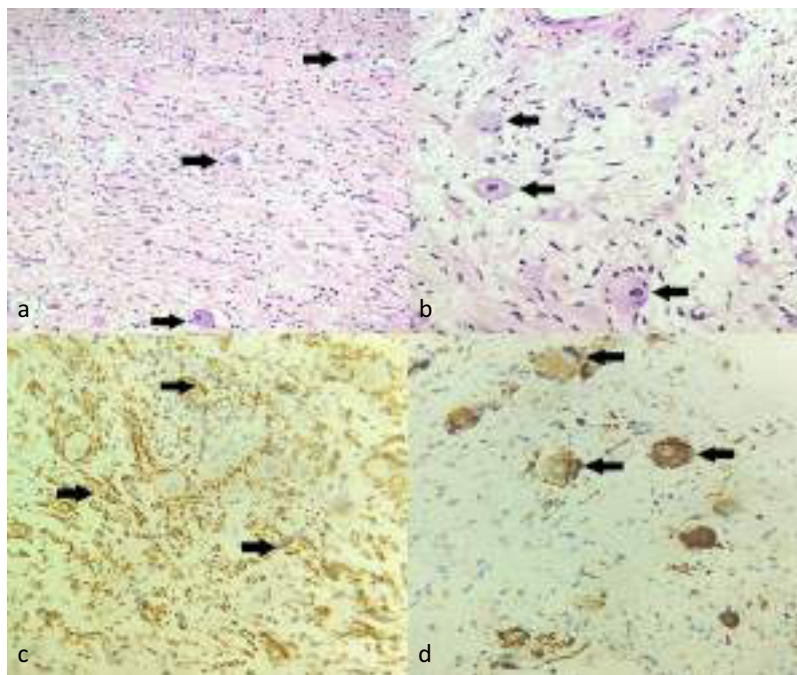
Fig. 6 – (A) Scattered large ganglion cells (arrowed) lie in a background of relatively low cellularity with a neural appearance. (B) Higher power occasionally ganglion cells with abundant pink cytoplasm are noted, one of which is bordered by satellite cells (arrowed). (C) Immunostain for GFAP highlights axonal processes, Schwann cells, and satellites (arrowed). (D) Immunoreactivity for synaptophysin highlights the ganglion cells (arrowed).

predominance in females with 1.5:1 ratio [10,11]. The reported incidence of GN is 1 per million population [12]. The most common locations for GN occurrence are the posterior mediastinum (41.5% of cases), retroperitoneum (37.5%), adrenal gland (21%), and neck (8%). Unusual sites include the spermatic cord, heart, bone, and intestine [9,10].

Retroperitoneal GNs are usually nonfunctioning and asymptomatic until they reach large size, in which case they cause symptoms due to local expansion and pressure on adjacent structures [13]. The compression of neighboring structures causes symptomatology such as back pain, abdominal pain, vomiting, constipation, weight loss, and urinary symptoms similar to our case presentation [14]. Although symptoms of autonomic dysfunction are usually seen in patients with hormone-secreting GNs, such symptoms may also occur in patients with paravertebral GNs compressing the autonomic fibers of the LS plexus [12].

The large lobulated mass lesion can be easily detected on conventional MRI. MRN adds incremental information in the diagnostic approach of such lesions. The high-resolution isotropic 3D and the superior contrast ability of the MRN image allow the multiplanar representation of the lesions, thus evaluating the size, presence of peritumoral edema, and enhancement after the contrast, and demonstrates the relationships of the involved and displaced nerve roots as in our case. In addition, diffusion-weighted imaging results in effective vascular signal and background suppression to demonstrate the extent of the tumor and internal cellularity. High ADC has been shown to be useful in diagnostic evaluation of nerve sheath tumors in confirming their benignity. The definitive diagnosis is provided by histological confirmation on biopsy or surgery [15–18].

GNs are usually circumscribed and occasionally show an irregular interface with soft tissue. Multiple GNs are rare [19]. On cut surface, they appear firm, light, and somewhat translucent. Histologically, multiple GNs consist of ganglion cells and axonal processes in large number accompanied by satellite cells and Schwann sheaths. The latter may be few in number compared with normal ganglia. Many are dysmorphic. Myelination is absent. The axonal processes and their ensheathment may lie loose-textured or in compact bundles. GNs often undergo degenerative changes, including vascular hyalinization, hemorrhage, cystic change, chronic inflammation, and stromal collagen deposition. Although well differentiated, the ganglion cells vary in size, often being multinucleate, and contain Nissl substance in varying quantity; axons and Schwann sheaths are often bundled in pseudofascicles. Cytoplasmic vacuoles, inclusions, and even features of neurodegenerative change such as Pick bodies maybe seen [20].

The association of GN with neurofibromatosis type 1 is well established. Familial but non–syndrome-associated examples are rare [21].

Typically, on CT, the lesion is seen as a well-circumscribed, solid, oval, or crescent shape, encapsulated masses that are isoattenuating to hypoattenuating to muscle. The lesion may also demonstrate calcifications (20%), which are typically fine and speckled, but may be coarse [22].

Reported MRI signal characteristics include homogeneous low or intermediate signal on T1-weighted, and heterogeneously intermediate or high signal on T2-weighted imaging and the post-gadolinium imaging showing variable none to heterogeneous enhancement [23].

Any improvement in the diagnostic accuracy of noninvasive imaging for characterizing the population of sheath tumors is valuable, given the high prevalence of benign lesions that may be unnecessarily referred for biopsy rather than follow-up [18].

The treatment of this type of tumor is essentially a surgical procedure. There are authors who advocate therapeutic abstinence when the diagnosis is made through biopsy, but biopsies are repeated if the tumor size increases to disguise the onset of neuroblastoma, or if there are symptoms or complications, such as root compression, mass effect, or increase in the secretory activity of catecholamines [14].

In conclusion, we present an illustrative case of retroperitoneal GN. Using MRN, the lesion was well evaluated with anatomic and diffusion characteristics indicating benignity. The histopathological examination confirmed the final diagnosis.

REFERENCES

[1] Robbins NM, Shah V, Benedetti N, Talbott JF, Chin CT, Douglas VC. Magnetic resonance neurography in the diagnosis of neuropathies of the lumbosacral plexus: a pictorial review. Clin Imaging 2016;40:1118–30.

[2] Papavramidis TS, Michalopoulos N, Georgia K, Kesisoglou I, Valentini T, Georgia R, et al. Retroperitoneal ganglioneuroma in an adult patient: a case report and literature review of the last decade. South Med J 2009;v(X):n–X.

[3] Miyake M, Tateishi U, Maeda T, Arai Y, Seki K, Hasegawa T, et al. A case of ganglioneuroma presenting abnormal FDG uptake. Ann Nucl Med 2006;20(5):357–60.

[4] Lonergan GJ, Schwab CM, Suarez ES, Carlson CL. Neuroblastoma, ganglioneuroblastoma and ganglioneuroma: radiologic-pathologic correlation. Radiographics 2002;22(4):911–34.

[5] Cejas C, Escobar I, Serra M, Barroso F. High resolution neurography of the lumbosacral plexus on 3 T magnetic resonance imaging. Radiología 2015;57(1):22–34.

[6] Chhabra A, Faridian-Aragh N. High-resolution 3-T MR neurography of femoral neuropathy. AJR Am J Roentgenol 2012;198(1):3–10.

[7] Soldatos T, Andreisek G, Thawait GK, Guggenberger R, Williams EH, Carrino JA, et al. High-resolution 3-T MR neurography of the lumbosacral plexus. Radiographics 2013;33(4):967–87.

[8] Chhabra A, Flammang A, Padua A Jr, Carrino JA, Andreisek G. Magnetic resonance neurography: technical considerations. Neuroimaging Clin N Am 2014;24(1):67–78.

[9] Koktener A, Kosehan D, Akin K, Bozer M. Incidentally found retroperitoneal ganglioneuroma in an adult. Indian J Surg 2015;77(1):S3–5. doi:10.1007/s12262-013-1030-1.

[10] Geoerger B, Hero B, Harms D, Grebe J, Scheidhauer K, Berthold F. Metabolic activity and clinical features of primary Ganglioneuromas. Am Cancer Soc 2001;29.

[11] Villaça J, Torres CM. Ganglioneuroma da região cervical. Mem Inst Oswaldo Cruz 1938;253–7.

[12] Shetty PK, Balaiah K, GnanaPrakash S, Shetty PK. Ganglioneuroma always a histopathological diagnosis. Health Allied Sci 2010;9(4):19.

[13] Zugor V, Amann K, Schrott KM, Schott GE. Retroperitoneales ganglioneurom. Aktuel Urol 2005;36:349–52. doi:10.1055/s-2004-830278.

[14] Martinho D, Pereira S, Formoso R, Barros P, Carvalho AP, Deus R, et al. Ganglioneuromaretroperitoneal: envolvimento do pedículo vascular do rim esquerdo. Acta Urol 2008;25(2):63–6.

[15] Vargas MI, Viallon M, Nguyen D, Beaulieu JY, Delavelle J, Becker M. New approaches in imaging of the brachial plexus. Eur J Radiol 2010;74(2):403–10. doi:10.1016/j.ejrad.2010.01.024. [Epub 2010 Mar 12]. PubMed PMID: 20223611.

[16] Viallon M, Vargas MI, Jlassi H, Lövblad KO, Delavelle J. High-resolution and functional magnetic resonance imaging of the brachial plexus using an isotropic 3D T2 STIR (short term inversion recovery) SPACE sequence and diffusion tensor imaging. Eur Radiol 2008;18(5):1018–23. doi:10.1007/s00330-007-0834-4. [Epub 2008 Jan 8]. PubMed PMID: 18180925.

[17] Chhabra A, Soldatos T, Subhawong TK, Machado AJ, Thawait SK, Wang KC, et al. The application of three-dimensional diffusion-weighted PSIF technique in peripheral nerve imaging of the distal extremities. J Magn Reson Imaging 2011;34(4):962–7.

[18] Demehri S, Belzberg A, Blakeley J, Fayad LM. Conventional and functional MR imaging of peripheral nerve sheath tumors: initial experience. AJNR Am J Neuroradiol 2014;35(8):1615–20.

[19] Shotton JC, Milton CM, Allen JP. Multiple ganglioneuroma of the neck. J Laryngol Otol 1992;106:277–8.

[20] Bender BL, Ghatak NR. Light and electron microscopic observations on a ganglioneuroma. Acta Neuropathol 1978;42:7–10.

[21] Robertson CM, Tyrrell JC, Pritchard J. Familial neural crest tumours. Eur J Pediatr 1991;150:789–92.

[22] Ichikawa T, Ohtomo K, Araki T, Fujimoto H, Nemoto K, Nanbu A, et al. Ganglioneuroma: computed tomography and magnetic resonance features. J Radiol 1996;69:114–21.

[23] Gahr N, Darge K, Hahn G, Kreher BW, von Buiren M, Uhl M. Diffusion-weighted MRI for differentiation of neuroblastoma and ganglioneuroblastoma/ganglioneuroma. Eur J Radiol 2011;79:443–6.